International Journal of Mechanical, Industrial and Aerospace Sciences
ISSN: 2517-9950
Vol:5, No:4, 2011

Oil Debris Signal Detection Based on Integral Transform and Empirical Mode Decomposition

Chuan Li and Ming Liang

***Abstract*—**Oil debris signal generated from the inductive oil debris monitor (ODM) is useful information for machine condition monitoring but is often spoiled by background noise. To improve the reliability in machine condition monitoring, the high-fidelity signal has to be recovered from the noisy raw data. Considering that the noise components with large amplitude often have higher frequency than that of the oil debris signal, the integral transform is proposed to enhance the detectability of the oil debris signal. To cancel out the baseline wander resulting from the integral transform, the empirical mode decomposition (EMD) method is employed to identify the trend components. An optimal reconstruction strategy including both de-trending and de-noising is presented to detect the oil debris signal with less distortion. The proposed approach is applied to detect the oil debris signal in the raw data collected from an experimental setup. The result demonstrates that this approach is able to detect the weak oil debris signal with acceptable distortion from noisy raw data.

***Keywords*—**Integral transform, empirical mode decomposition, oil debris, signal processing, detection.

I. Introduction

Oil debris monitors (ODMs) have been widely used to diagnose the healthy conditions of oil-lubricated systems [1]. Once a metallic particle in lubricating oils passes through the sensor tube, a single period sine-like characteristic signal appears at the output of the ODM. The signal phase difference between a ferromagnetic and a non-ferromagnetic particle is 180°. The amplitude of the characteristic signal is proportional to the mass of the ferromagnetic particle and to the surface area of the non-ferromagnetic one as long as the flow rate is approximately constant. Taking both the phase and the amplitude into account, the ODM is able to estimate the size and the distribution of the wear debris in the lubricating system and to accordingly detect the early fault of the machinery system [2].An ODM sensor is often installed on the return line of the hydraulic circuit to detect the presence of the particle. Besides the sensitivity to the metallic particles, the sensor also picks up vibration signals generated by the mechanical system. The weak particle signal is often deep covered by the mixture of the vibration interference and other random noise and thus cannot be observed directly. Much effort has been made to detect the weak signal from the severely contaminated ODM data. Aiming at improving the responsiveness to early machine failures and reducing the false alarms, Fan et al [3] suggested a method based on both wavelet transform and kurtosis analysis to address these two issues simultaneously. The test results have demonstrated that this method could effectively detect very weak particles signals buried in strong background noise and eliminate vibration-like spurious signals. Hong and Liang [4] proposed a fractional calculus technique consisting of two detectors for on-line detection of oil debris. This technique does not require any additional filtering or de-noising steps, and signal processing can be simplified accordingly. Bozchalooi and Liang [5] developed a two-stage de-noising scheme including wavelet-based adaptive subband filtering and thresholding. Both simulated and experimental data demonstrated the enhancement of the ODM performance with this scheme. A low-pass filter and empirical mode decomposition (EMD) was also suggested by Bozchalooi and Liang [6] to extract particle signatures from the output of oil debris sensors. The proposed algorithm has been tested using both simulated and experimental data and has shown to be effective. Though these studies are quite effective in detecting of the presence of particles, they may not be suited for particle size estimation cannot be used to reliably estimate the particle size largely due to the filtering process that often alter the particle signature.For most of signal detection cases, the prior knowledge of the signal or the noise is unavailable. Hence the authenticity of extracted signal cannot be validated, or at least, cannot be validated during the detection process. Fortunately, the oil debris signature is unique, featuring sine-like profile, as well as sparse, randomly appearing and low frequency signal. Considering such prior knowledge of the oil debris signal, we propose a joint integral transform and empirical mode decomposition (ITEMD) approach to extract fine particle signal and to estimate particle size. The paper is organized as follows. Section II explains how the oil debris signal can be enhanced using integral transform. This is followed by trend component identification from the intrinsic mode functions (IMFs) of the EMD, which is detailed in section III. An optimal signal reconstruction procedure is proposed in section IV. Section V presents the experimental work. Conclusions are drawn in section VI.

II. Oil Debris Signal Enhancement Using Integral Transform

As mentioned above, the raw data of the ODM is usually the mixture of three components: oil debris signal, vibration induced noise and random noise, i.e.,

$$r(t) = s(t) + v(t) + n(t) \quad (1)$$

where $r(t)$, $s(t)$, $v(t)$ and $n(t)$ respectively denotes raw data, oil debris signal, vibration noise and random noise. Suppose that in a specific time interval $[T_a, T_b]$ there is an ideal particle signal $s(t)$ which can be expressed as

Chuan Li is currently with Department of Mechanical Engineering, University of Ottawa, Ottawa K1N 6N5, Canada. (e-mail: chuanli@21cn.com)
Ming Liang is with Department of Mechanical Engineering, University of Ottawa, Ottawa K1N 6N5, Canada. (*corresponding author. phone: 613-562-5800 ext. 6269; e-mail: ming.liang@uottawa.ca)

$$s(t)=\begin{cases} a\sin(2\pi ft-T_0); t\in[T_0,T_0+1/f] \\ 0; \text{otherwise} \end{cases} \quad (2)$$

where f is the particle signal frequency, $[T_0, T_0+1/f]$ the particle signal passing period, and a the signal amplitude. If a is positive for a ferromagnetic particle then it is negative for a non-ferromagnetic one. Suppose that the flow rate of the oil is in the range $[F_{min}, F_{max}]$, the sensor tube diameter is D and the distance between two field coils is d. The particle signature frequency f is bounded by [3]

$$f\in\left[\frac{4F_{\min}}{\pi D^2 d},\frac{4F_{\max}}{\pi D^2 d}\right] \quad (3)$$

In practice, the maximal frequency of the particle signal is often less than 50Hz, which is lower than most of frequencies of vibration interferences with larger amplitude.

The ODM works in response to the inductive change caused by passing metallic particles [7], which means that it is also sensitive to the vibration velocity of the oil line on which the sensor is mounted. The vibration induced interference signal $v(t)$ is approximately proportional to the vibration velocity. For the convenience of the analysis, the dominant component of the vibration velocity can be simplified as a sinusoidal signal

$$v(t)=b\sin 2\pi pt \quad (4)$$

where b and p are respectively the vibration amplitude and frequency. It is obvious that the vibration displacement $x(t)$ is the integral of the velocity, i.e.

$$x(t)=\int v(t)\mathrm{d}t=\frac{-b}{2\pi p}\cos 2\pi pt \quad (5)$$

The random noise is generally much weaker than the vibration interference and thus neglected. To quantify the "quality" of a oil debris signal dataset and to evaluate the performance of the proposed method, we define the particle-to-vibration ratio (PVR) of the raw signal $r(t)$ as

$$PVR(r)=\frac{s(t)\big|_{p-p}}{v(t)\big|_{p-p}} \quad (6)$$

where the subscript 'p-p' represents the peak-to-peak value. A high PVR indicates good signal quality, i.e., good particle detectability. Thus, our goal is to improve the PVR. This can be done by the integral transform of the oil debris signal. The PVR of the transformed signal is

$$PVR(I(r))=\frac{\left(\int s(t)\mathrm{d}t\right)_{p-p}}{\left(\int v(t)\mathrm{d}t\right)_{p-p}}=\frac{p}{f}PVR(r) \quad (7)$$

where $I(.)$ represents the integral transform. Since most of vibration interference frequencies are much higher than the frequency of the particle signal, i.e. $n>p$, The above equation shows that the PVR can be improved by p/f times using the simple integral transform.

To demonstrate the effectiveness of the above method, we simulate a signal according to (1) as

$$\begin{cases} r(t)=s(t)+v(t)+n(t) \\ s(t)=\begin{cases} 0.8\sin(70\ \pi t-0.25); & t\in[0.25,0.25+1/35] \\ 0; & \text{other} \end{cases} \\ v(t)=1.5\sin(978\pi t)+1.8\sin(817\pi t) \\ n(t)=\mathrm{rnd}(0.5) \end{cases} \quad (8)$$

where $t\in[0,1]$, rnd(.) denotes the random number $\in[-0.5,0.5]$. The sampling frequency is set as 8kHz. Fig. 1(a) displays the simulated raw data $r(t)$. Due to the interference from $v(t)$ and $n(t)$, the signal $s(t)$ cannot be observed directly. To compare, we integral transform the raw data and obtain $r_1(t)=I(r(t))$ as shown in Fig. 1(b). It is obvious that the particle-to-vibration ratio is improved significantly.

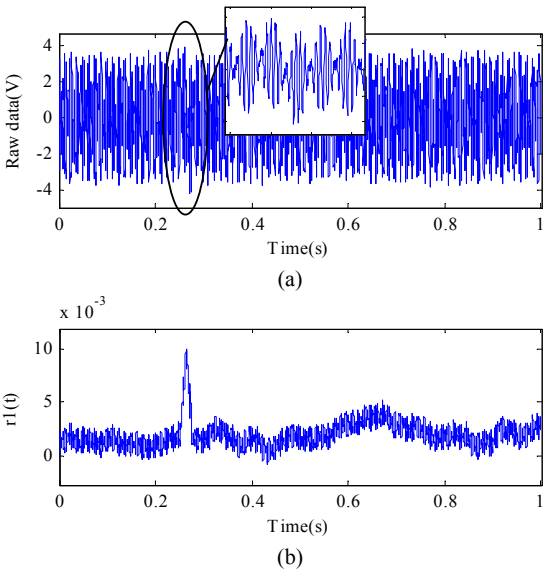

Fig. 1 (a) Simulated raw data, and (b) integral transformed data.

However, to accurately estimate particle size, the high frequency noise mixed with the oil debris signal and the trend component (baseline wander) have to be removed from the integral transformed signal. The removal of these signal components is detailed in the next section.

III. Removal of Trend and High Frequency Components

A. Trend removal

The baseline drifting resulting from data acquisition error and other causes may be insignificant in many cases but is often

worsened by the integral transform. Therefore, it has to be removed. We propose using EMD for this purpose because EMD is highly adaptive and require minimal pre-specified parameters. With the EMD [8], the signal is decomposed into several elementary intrinsic-mode functions (IMFs). For example, the integral transformed signal $r_1(t)$ can be adaptively decomposed as

$$r_1(t) = \sum_{i=1}^{I} IMF_i(t) + RS(t) \tag{9}$$

where I is the decomposition levels, $IMF_i(t)$ ($1 \le i \le I$) denotes the ith IMF, and $RS(t)$ represents the residue which is regarded as the last 'IMF' ($IMF_{i+1}(t)$) in this paper for the convenience of analysis in the context.

The EMD result of the integral transformed signal in Fig. 1(b) is plotted in Fig. 2. It consists of eight IMFs and a residue (IMF_9).

Due to the low-frequency feature, the trend components may spread over the last several IMFs and the residue. It is well-known that trend components exist if the associated IMFs are of zero mean, and no trend otherwise. Therefore trend can be identified by looking at the IMF means. More specifically, if order i of an IMF is equal to or greater than trend order J, the IMF should be the trend IMF and accordingly be set to zero to remove the trend components. In our research, the trend order J is determined if: 1) $\sum_{i=1}^{T-1} \left|\text{mean}\,(IMF_i(t))\right| \le \left|\text{mean}\,(IMF_T(t))\right|$; and 2) for all the order $J \le j \le i+1$, inequality $\sum_{i=1}^{j} \left|\text{mean}\,(IMF_i(t))\right| \le \left|\text{mean}\,(IMF_j(t))\right|$ always holds.

According to the aforementioned procedure, the trend order of the EMD of $r_1(t)$ shown in Fig. 2 is calculated as 8, which means that the trend components reside mainly in IMF_8 and the residue (IMF_9).After determining the trend order J, one can directly remove trend IMFs from the original signal since the trend IMFs usually possesses less information of the target signal [9]. The de-trended signal, $r_2(t)$ can be expressed as

$$r_2(t) = r_1(t) - \sum_{i=J}^{I+1} IMF_i(t) = \sum_{i=1}^{J-1} IMF_i(t) \tag{10}$$

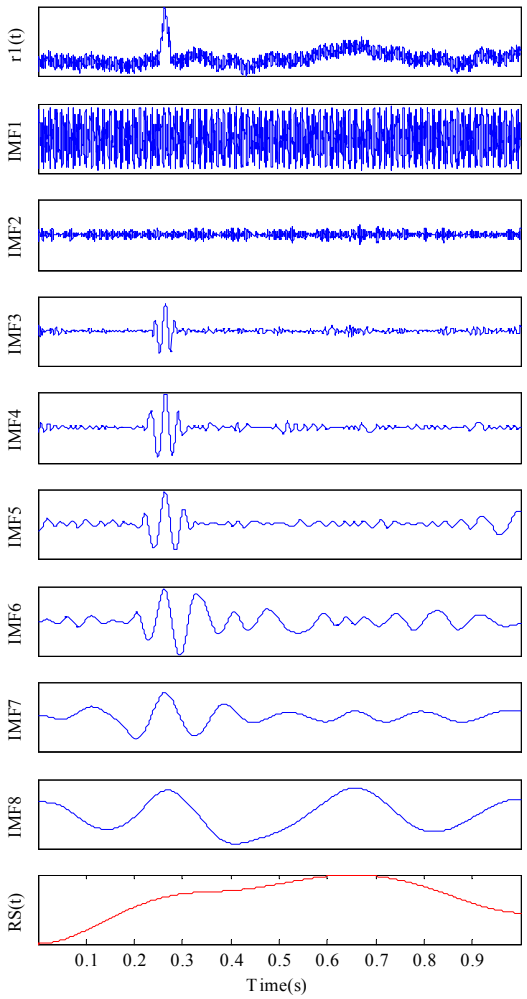

Fig. 2 The IMFs and residue of the integral transformed signal shown in Fig. 1(b) (The vertical axes of plots are not in the same scale).

The comparison between the integral transformed data $r_1(t)$ and the de-trended data $r_2(t)$ (=$r_1(t)$-IMF_9-IMF_8) is shown in Fig. 3. It is shown that the baseline wander of $r_1(t)$ has been mostly eliminated.

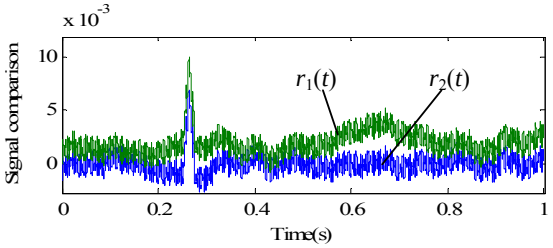

Fig. 3 Comparison between the integral transformed data $r_1(t)$ (also shown in Fig. 1(b)) and the de-trended data $r_2(t)$.

B. High frequency component removal

To eliminate the high frequency signal components, the mode cell [10], i.e., the oscillatory cell between two zero-crossings, is used as the basic thresholding unit. To partially reconstruct the signal from coarse to fine [11], there are J-1 reconstructions to be evaluated. The kth reconstruction, $R_k(t)$, is given by

$$R_k(t) = \sum_{k}^{J-1} IMF_k(t) \tag{11}$$

The mode cell E_k^i In each reconstruction order k, can be thresholded by [12]

$$H_k = \sigma_k \sqrt{2\ln(L)} \tag{12}$$

where L is the length of the measured data, σ_k the standard deviation of $R_k(t)$. In mode cell thresholding, the whole mode cell E_k^i is preserved as long as at least one point of the mode cell survives the H_k thresholding. This operation does not only preserve the integrity of the EMD oscillatory mode, but also help to minimize signal distortion.

Fig. 4 demonstrates all the partial reconstruction results for $r_2(t)$ shown in Fig. 3. As displayed in Fig. 4, there are four reconstructions available. Which of the four options is selected for reconstruction will lead to different levels of signal distortion. An optimal selection process is explained in the next section.

IV. Optimal Signal Reconstruction

Considering the fact that the minimal signature distortion means maximal correlation with the ideal signal, a correlation coefficient (CC) reflecting both waveform area and profile is defined to select the best reconstruction order that yields the minimal waveform distortion. The CC between an option E_k^i and the target signature is given by

$$\rho_k^i = \frac{A_k^i}{A_{\max}^i} \times \frac{\mathrm{COV}((E_k^i)', (G_k^i)')}{\sqrt{\mathrm{D}((E_k^i)') \bullet \mathrm{D}((G_k^i)')}} \tag{13}$$

where ρ_k^i is the CC between option E_k^i and the target estimation G_k^i, COV(·) represents covariance function, D(·) represents variance function, (·)' denotes the differention operator, A_k^i is the waveform area associated with option E_k^i, and $A_{\max}^j$ is its target area, which is given by

$$A_{\max}^i = \max\left(A_1^i, A_2^i, \ldots, A_{J-1}^i\right) \tag{14}$$

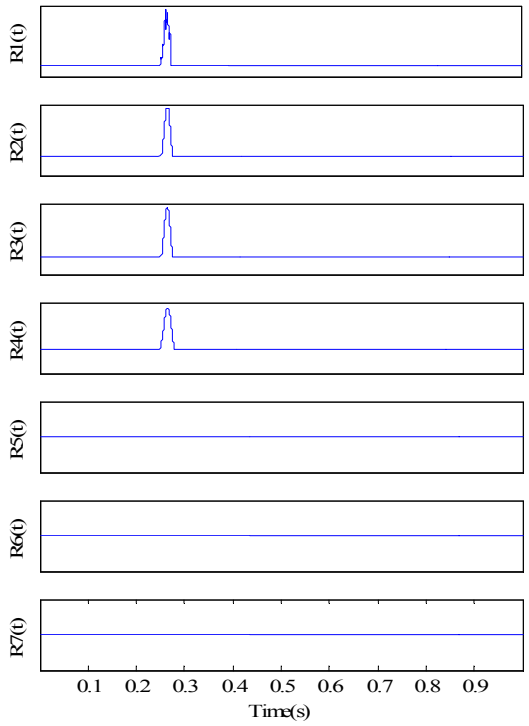

Fig. 4 Partial signal reconstruction results based on the mode cell thresholding.

Suppose that the target signal has the same area as that of E_k^i, i.e.,

$$\int_{i_1}^{i_N} G_k^i \mathrm{d}t = A_k^i \tag{15}$$

where i_1 and i_N are two zero-crossings of the mode cell E_k^i.

The target area can be obtained by (2) and (15).

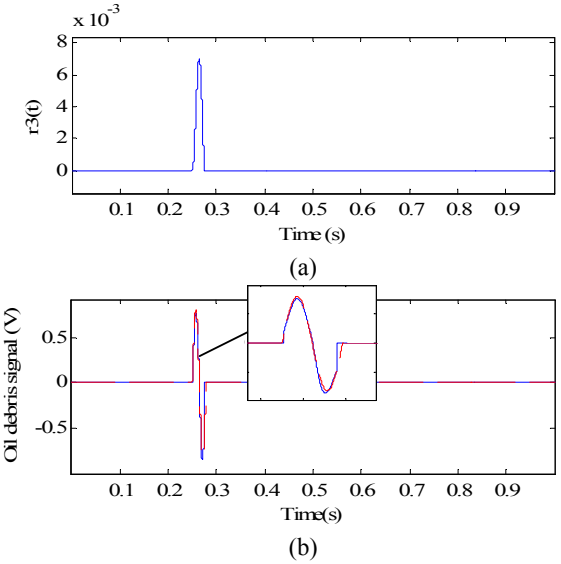

Fig. 5 Optimal reconstruction results: (a) optimal reconstruction $r_3(t)$, and (b) comparison between $r_3'(t)$ (the differentiated $r_3(t)$, solid line) and $s(t)$ (dashed line, given by (8)).

Obviously, the option associated with the highest CC should be selected as optimal reconstruction $r_3(t)$. Then, a differential transform (i.e., inverse integral transform) is perform for $r_3(t)$ to obtain $r_3^{'}(t)$, the optimal estimation of the oil debris signal $s(t)$. According to the calculation for reconstructions shown in Fig. 4, $R_2(t)$ (=IMF_7+IMF_6+IMF_5+IMF_4+IMF_3+IMF_2) including the mode cell E_2 has the maximal CC and thus is selected as the optimal reconstruction $r_3(t)$. Fig. 5 describes the reconstruction results. The results shows that the optimal estimation $r_3^{'}(t)$ is very close to the target oil debris signal $s(t)$.

V. Experimental Evaluation

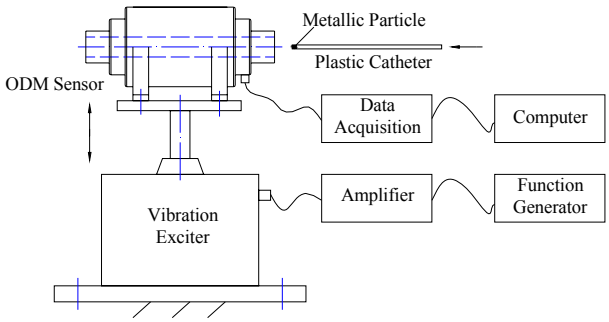

Fig. 6 Experimental setup

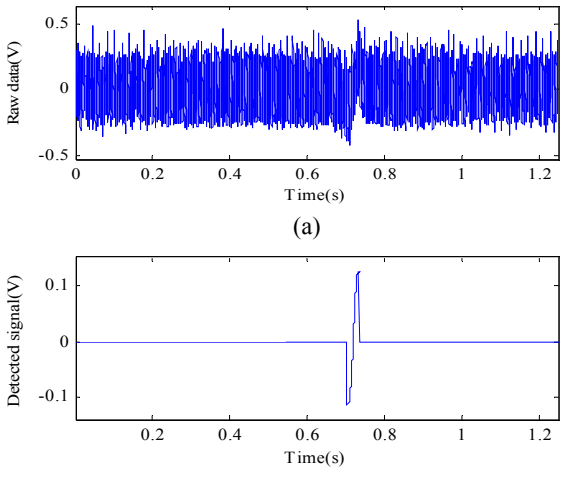

Fig. 7 Experimental results. (a) signal measured from the ODM sensor when a nickel particle is manually passed through the tube, and (b) the detected oil debris signal.

To evaluate the performance of the proposed method, an ODM sensor is mounted on a vibration exciter driven by a function generator and an amplifier. As shown in Fig. 6, a small nickel particle (roughly 40-50μm in diameter) is embedded in a plastic catheter which is manually led through the tube of the sensor to generate the oil debris signal. Due to the intrinsic characteristics, the random noise is unavoidable for the setup shown in Fig. 6. The mixture of the oil debris signal, the vibration noise and the random noise is captured by a computer through a data acquisition card.The sampling frequency is set at 8 kHz. Fig. 7(a) shows part of the raw data collected from the setup. Fig, 7(b) displays the extracted oil debris signal which is very similar to the target signal. This clearly demonstrated the effectiveness of the proposed approach in detecting weak oil debris signal from contaminated raw data collected by the ODM sensor.

VI. Conclusion

This paper reports a new method to detect the weak oil debris signal from the severely contaminated raw data. The integral transform is first employed to enhance the detectability of the metal particle signature. The enhanced signal is then adaptively decomposed into several IMFs by the EMD to remove the baseline wander caused by the integral transform step. Considering the intrinsic features of the oil debris signal, the mode cell thresholding and the maximal correlation coefficient reconstruction are presented to find the optimal reconstructed signal. A simulation case reveals that the detected signal using the proposed ITEMD approach is very close to the ideal signal. This method is also validated using the experimental data.

Acknowledgment

This work is supported in part by the Natural Sciences and Engineering Research Council of Canada and Ontario Centers of Excellence.

References

[1] S. Greenfield, "Oil debris monitoring for the Eurofighter 2000 aircraft," *Proceedings of Condition Monitoring 2001 Conference*, Oxford, England, pp. 254-266, Jun. 2001.

[2] J. L. Miller and D. Kitaljevich, "In-line oil debris monitor for aircraft engine condition assessment," *2000 IEEE Aerospace Conference Proceedings*, vol. 6, pp. 49-56, Mar. 2000.

[3] X. Fan, M. Liang and T. Yeap, "A joint time-invariant wavelet transform and kurtosis approach to the improvement of in-line oil debris sensor capability," *Smart Materials & Structures*, vol. 18, no. 8, pp. 085010, Aug. 2009.

[4] H. B. Hong and M. Liang, "A fractional calculus technique for on-line detection of oil debris," *Measurement Science & Technology*, vol. 19, no. 5, pp. 055703, May 2008.

[5] I. S. Bozchalooi and M. Liang, "In-line identification of oil debris signals: an adaptive subband filtering approach," *Measurement Science & Technology*, vol. 21, no. 1, pp. 015104, Jan. 2010.

[6] I. S. Bozchalooi and M. Liang, "Oil debris signal analysis based on empirical mode decomposition for machinery condition monitoring," *Proceedings of American Control Conference 2009*, vol. 1-9, pp. 4310-4315, Jun. 2009.

[7] R. W. Kempster and D. B. George, "Method and apparatus for detecting particles in a fluid having coils isolated from external vibrations," *U.S. patent No. 5,444,367*, 1995

[8] N. E. Huang, Z. Shen, S. R. Long, M. L. Wu, H. H. Shih, Q. Zheng, N. C. Yen, C. C. Tung and H. H. Liu, "The empirical mode decomposition and Hilbert spectrum for nonlinear and nonstationary time series analysis," *Proc. Roy. Soc. Lond. A*, vol. 454, no. 1971, pp. 903–995, Mar. 1998.

[9] Z. H. Wu, N. E. Huang, S. R. Long and C. K. Peng, "On the trend, detrending, and variability of nonlinear and nonstationary time series," Proceedings of the National *Academy of Sciences of the United States of America*. vol. 104, no. 38, pp. 14889-14894, Sep. 2007.

[10] C. S. Qu, T. Z. Lu and Y. Tan, "A modified empirical mode decomposition method with applications to signal de-noising," *Acta Automatica Sinica*, vol. 36, no. 1, pp. 67-73, Jan. 2010.

[11] B. N. Krupa, M. A. M. Ali and E. Zahedi, "The application of empirical mode decomposition for the enhancement of cardiotocograph signals," *Physiological Measurement*, vol. 20, no. 8, pp. 729-743, Aug. 2009.

[12] S. G. Mallat, "A wavelet tour of signal processing," *San Diego: Academic*, 1998.